Spatial and Temporal Distributions of a Gaseous Pollutant During Simulated Preventive Maintenance and Pipe Leaking Events in a Working Cleanroom

Shih-Hsuan Huang, Hui-Ya Shih, Shou-Nan Li, Sheng-Chieh Chen, and Chuen-Jinn Tsai

***Abstract*—Sulfur hexafluoride (SF_6) of $> 99.9\%$ in purity was artificially released to simulate the emission sources in the etching/thin-film area of a working cleanroom in a semiconductor fab at the rate of 492 g/h. The temporal and spatial dispersion patterns of the gas pollutant were studied during the simulated preventive maintenance (PM) and pipe leaking exhaust events experimentally and numerically. Three mobile Fourier transform infrared spectrometers (FTIRs, detection limit: 10 ppb) were used simultaneously to measure the real time SF_6 concentrations in different locations of the etching/thin-film area of the cleanroom. An additional open-path FTIR with very low detection limit of 0.4 ppb was installed before the recirculation duct in the lithography area to monitor if the pollutant drifted from the etching/thin-film area to the lithography area. The results show that the 3-D numerical model predicts the unsteady gas concentration accurately in both the peak concentration and the time required to reach the peak concentration. Due to high dilution of the pollutant in the cleanroom, the current gas sensors may not be sensitive enough and a better monitoring system and strategy is needed to protect workers from injury and ensure good product yield. The well-mixed model predicts the peak pollutant concentrations within a reasonable range which is 0.34–1.33 times the experimental values except when the monitored distance is very close to the release point. Although it is not able to predict the time required to reach the peak concentration and the time for the concentration to drop below a small level, the simple well-mixed model can be used to obtain an estimation of the peak concentration quickly when the emission rate and the ventilation condition of the cleanroom are different than the current study.**

***Index Terms*—Airborne molecular contamination, cleanroom, gas sensors, preventive maintenance.**

I. Introduction

AIRBORNE contaminants pose a serious threat to the state-of-the-art manufacturing processes as the feature size continues to shrink in the semiconductor industry. When a gas pollutant leaks from the pipes, fittings or process chambers, it mixes with the recirculation air and disperses in the cleanroom to become an airborne molecular contamination (AMC), which will cause process tool damage, product corrosion, wafer defects and potential worker injury [1].

Many micro-contamination studies in the cleanroom have been conducted in the past. When the concentration of hydrogen chloride was higher than 28 ppb, the corrosion defects were observed on the test wafer [2]. The concentration of ammonia of 20 ppb could cause the critical dimension shift of 25%–35% depending on the type of photoresists [3]. When chemically amplified resist was left in an uncontrolled atmosphere of about 10 ppb NH_3, patterns on the wafers were either not developed or T-top phenomenon occurred [4]. Hazy optical lens were found in a TFT-LCD fab due to the continuous emission of high concentration of NH_3 into the cleanroom during the preventive maintenance (PM) process of the photo-resist stripper [5]. Ruthenium (Ru) airborne contaminant, which diffused to the cleanroom during cleaning of Ru CVD furnace tubes, was determined as a harmful gas to the MOSFETs process [6]. High concentrations of corrosive and toxic gases were found to emit from the metal etch chambers and downstream pipelines during PM process [7], [8]. Without appropriate control, hydrogen chloride (HCl) as high as 343 ppm was detected inside the enclosed chamber, which might cause corrosion on the wafers and the process tools after the chamber was opened. Therefore, to ensure high yield manufacturing in semiconductor industry, the pollutant concentration must be controlled below a certain limit. For example, the yield enhancement committee of the International Technology Roadmap for Semiconductors (ITRS) recommended that the concentration of the total inorganic acids and bases be less than 0.5 and 2.5 ppb, respectively, for reticle exposure environment, or less than 5.0 and 50.0 ppb, respectively, for lithography clean room environment for the year 2007-2015 [9]. To meet this stringent requirement, chemical filters are often used to reduce the AMC concentration in the cleanroom [2]–[4]. Mini-environment and SMIF (standard mechanical interface) enclosure are also useful tools to achieve the requirement of cleanliness [10]. An effective ventilation control during preventive maintenance is an important method method to reduce AMC contamination in the cleanroom [8].

However, AMC concentration in the clean room is nonuniform and unsteady which requires an in-depth study. Chen *et al.* [11] studied the detailed flow and transient concentration fields of a gaseous pollutant emitted from a valve manifold box experimentally and numerically. Hot spots of the pollutant, the peak concentration and the time taken for reducing the pollutant concentration to the background level were found. This study used the similar experimental and numerical methods of Chen *et al.*

Manuscript received September 23, 2008; revised March 05, 2009; accepted March 06, 2009. First published July 07, 2009; current version published August 05, 2009.

S.-H. Huang, S.-C. Chen, and C.-J. Tsai are with the Institute of Environmental Engineering, National Chiao Tung University, Hsinchu, Taiwan (e-mail: cjtsai@mail.nctu.edu.tw; shhuang.ev94g@nctu.edu.tw; shawn.ev93g@nctu.eud.tw).

H.-Y. Shih and S.-N. Li are with the Energy and Environment Research Laboratories, Industrial Technology Research Institute (ITRI), Hsin Chu, Taiwan (e-mail: HuiYaShih@itri.org.tw; SNLi@itri.org.tw).

Digital Object Identifier 10.1109/TSM.2009.2024874

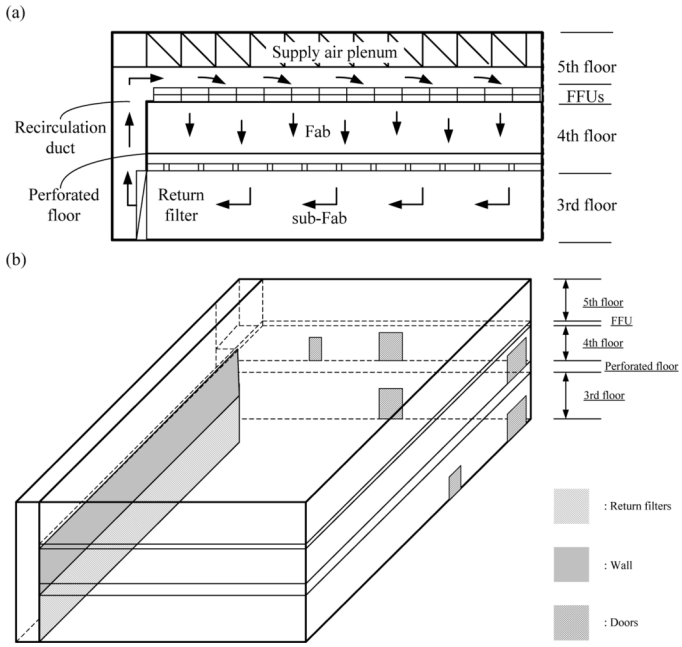

Fig. 1. (a) 2-D schematic diagram and air flow pattern in the FFU type cleanroom. (b) 3-D schematic diagram of the locations of the outlets.

[11] to investigate the spatial and temporal dispersion patterns of the gaseous pollutant in a working cleanroom during simulated preventive maintenance and gas leaking events. The possibility of cross-contamination of different working areas was also examined. The suitability of gas sensors and the applicability of the well-mixed model for predicting the pollutant concentration were then discussed in light of the dilution factors found in this study.

II. Experimental Method

The experimental study was conducted in a class 1, fan-filter-unit (FFU) type working cleanroom in one of the DRAM semiconductor fabs in Hsin Chu, Taiwan. Fig. 1(a) and (b) shows the 2-D and 3-D schematic diagrams of the cleanroom., in which the third, fourth, and fifth floor of the plant are sub-fab layer, fab layer and supply air plenum, respectively. The airflow is driven by 1900 FFUs which are located at the ceiling of the fab layer. The FFUs were group into 65 regions and the air velocities at 0.3 m below the FFUs were measured by a TSI Model 8330 anemometer (TSI, Inc., St. Paul, MN) at ten different points in each region. The flow rate of the make-up air is 168 448 CMH $(\mathrm{m}^3/\mathrm{h})$, or 4.7 air exchanges per hour.

Fig. 2 shows the layout of the fab layer, in which the static pressure is 1.1, 1.1, 1.2, and 1.8 mm $\mathrm{H_2O}$ in the etching, the thin film, the furnace and the lithography areas, respectively. The static pressure of the lithography area is higher than other areas and is expected to be cleaner. Since the lithography area has the cleanest requirement in the fab, the possibility of cross contamination to the lithography area from the etching/thin-film area was investigated in this study.

The two main sources of the AMCs in the cleanroom are preventive maintenance and pipe leaking, these two scenarios were studied experimentally. Additional numerical simulation of the gas pollutant dispersion was performed for the scenario A and

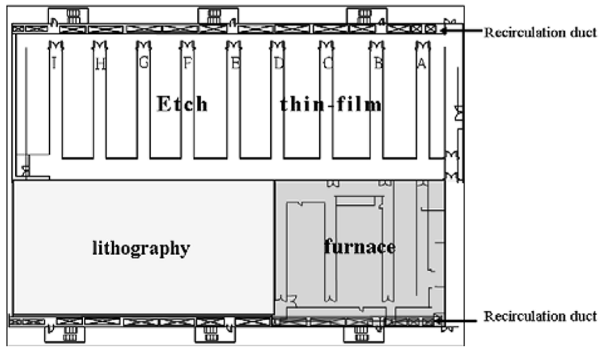

	W(width) x H(height) x L(length)		
Etching area	32m	16m	35m
Thin-film area	32m	16m	35m
Furnace	32m	16m	30m
Lithography	32m	16m	40m

Fig. 2. Layout and dimension of different working zones of the fab layer.

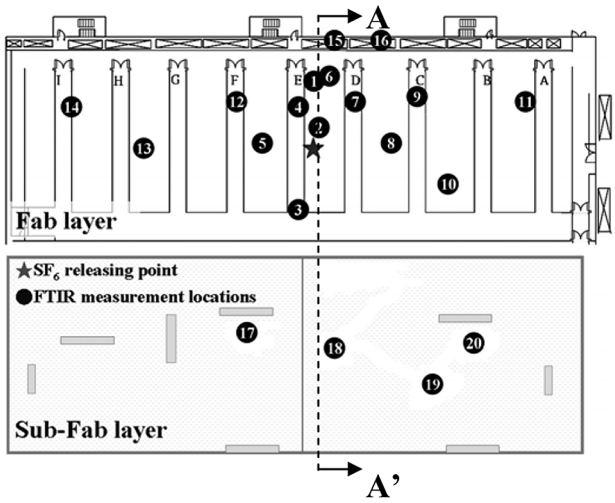

Fig. 3. Locations of the $\mathrm{SF_6}$ source and the measurement points in the etching/thin-film area, scenario A.

the simulated pollutant concentrations were compared with the experimental data.

A. Scenario A: Simulated Pollution Source From a Model Process Chamber

A simulated contamination source was set up in the maintenance zone between D and E working zones in the etching/thin-film area of the fab layer, as shown in Fig. 3. Sulfur hexafluoride $(\mathrm{SF_6})$ was used as the simulated gaseous pollutant because it is inactive and harmless to human health and wafer manufacture process. The flow rate of the $\mathrm{SF_6}$ gas ($> 99.9\%$ in purity, Air Products San Fu Co. Ltd., Taiwan), 1.35 L/min, was controlled by a mass flow controller (Model No. 5850E, Brooks Instrument, Austin, TX) and released from 24 evenly distributed holes $(\mathrm{ID} = 2\ \mathrm{mm})$ on a circular 1/4-in teflon tube placed at the bottom of the model chamber. The total $\mathrm{SF_6}$ mass emission rate was 492 g/h. The gas discharged from the teflon tube was

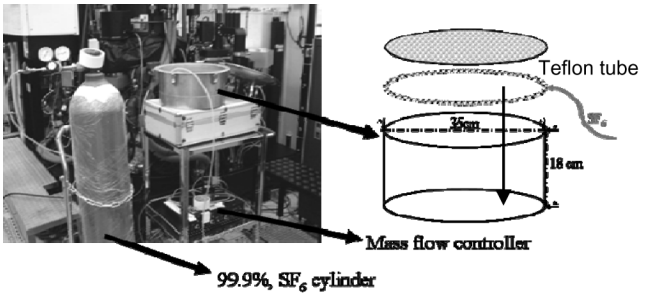

Fig. 4. Simulated SF_6 pollutant source from a model chamber.

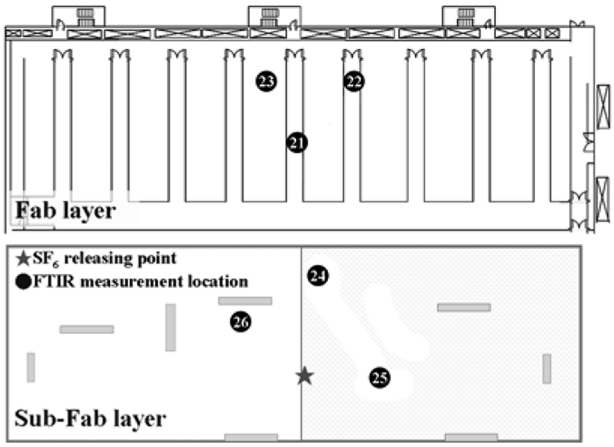

Fig. 5. Locations of the SF_6 source and the measurement points, scenario B.

passed through a screen near the top of the chamber to improve flow uniformity, as shown in Fig. 4. SF_6 gas was released for 10 min continuously then stopped.

Three mobile FTIRs (Work IR-104, ABB Bomem, Quebec, Canada) with a detection limit of 10 ppb were used simultaneously at three different locations to quantify the SF_6 concentration in the etching/thin-film areas for 10 min during 10-min SF_6 release and another 40 min after SF_6 release stopped. The monitoring points were located 1 m above the perforated floor and SF_6 concentrations were recorded every eight seconds by the three FTIRs. There were 20 measurement points (No. 1–20), 16 of them were on the fab layer and the other four on the sub-fab layer, as shown in Fig. 3. After one single experiment, the three FTIRs were moved to different measurement points and the experiments were repeated until all 21 points were measured.

B. Scenario B: Simulated Leaking Pipe From the Outlet Connector of a Dry Pump

Simulated SF_6 leaking at a rate of 1.35 L/min was conducted at the location of a dry pump through a 1/4-in Teflon tube, pointed upward with the opening 1 m above the ground. There were six measurement points (No. 21–No. 26), three of which were on the fab layer and the other three were on the sub-fab layer. The concentration of SF_6 was measured in the same way as in scenario A.

C. Cross Contamination Study

To determine if cross-contamination of different working zones occurred, an additional open-path FTIR with a very low detection limit of 0.4 ppb was used to monitor the SF_6 concentrations before the recirculation air unit of the lithography area during the experiments of both two scenarios. SF_6 concentration was taken once every 5 min and 10 data were obtained during each single 50-min experiment.

III. Numerical Method

In the numerical study, the mass and momentum conservation equations were solved by the commercial software, STAR-CD (version 3.24, CD-adapco Japan CO., Ltd). Assuming that the flow is steady and incompressible, the mass and momentum conservation equations are [12]:

$$\frac{\partial}{\partial x_j}(\rho u_j) = 0 \tag{1}$$

$$\frac{\partial}{\partial x_j}(\rho u_j u_i - \tau_{ij}) = -\frac{\partial p}{\partial x_i} \tag{2}$$

where x is the coordinate (m), subscripts i and j are the index of Cartesian components, u is the fluid velocity (m/s), ρ is the mass density $(\mathrm{kg/m^3})$, τ_{ij} is the stress tensor $(\mathrm{N/m^2})$, and p is the static pressure (Pa).

Standard $k-\varepsilon$ high Reynolds number model was used for simulating the turbulent flow in the cleanroom and the following two additional equations for k and ε were solved:

$$u_j\frac{\partial k}{\partial x_j} = \frac{1}{\rho}\frac{\partial}{\partial x_j}\left[\left(\mu+\frac{\mu_t}{\sigma_k}\right)\frac{\partial k}{\partial x_j}\right] + \frac{\mu_t}{\rho}\left(\frac{\partial u_i}{\partial x_j}+\frac{\partial u_j}{\partial x_i}\right)\left(\frac{\partial u_i}{\partial x_j}\right) - \varepsilon \tag{3}$$

$$u_j\frac{\partial \varepsilon}{\partial x_j} = \frac{1}{\rho}\frac{\partial}{\partial x_j}\left[\left(\mu+\frac{\mu_t}{\sigma_\varepsilon}\right)\frac{\partial \varepsilon}{\partial x_j}\right] + C_{\varepsilon 1}\frac{\varepsilon}{k}\frac{\mu_t}{\rho}\left(\frac{\partial u_i}{\partial x_j}+\frac{\partial u_j}{\partial x_i}\right)\left(\frac{\partial u_i}{\partial x_j}\right) - C_{\varepsilon 2}\frac{\varepsilon^2}{k} \tag{4}$$

where μ_t is the turbulent viscosity $(\mathrm{Ns/m^2})$ defined as $\mu_t = C_\mu \rho k^2/\varepsilon$. The values assigned in the standard $k-\varepsilon$ turbulence model coefficients: C_μ, $C_{\varepsilon 1}$, $C_{\varepsilon 2}$, σ_k, and σ_ε are 0.09, 1.44, 1.92, 1.0, and 1.22, respectively.

STAR-CD is based on the finite volume discretization method. The pressure-velocity linkage is solved by the SIMPLE (semi-implicit method for pressure linked equation) algorithm [13] and the differencing scheme for the space discretization method is the UD (upwind differencing) scheme. After the steady flow field was obtained, the unsteady SF_6 concentration field was calculated based on the mass conservation equation. The concentration of each constituent k in a fluid mixture, which is expressed as the mass fraction m_k, is governed by the following:

$$\frac{\partial}{\partial t}(\rho m_k) + \frac{\partial}{\partial x_j}(\rho u_j m_k - F_{k,j}) = 0 \tag{5}$$

where $F_{k,j}$ is its diffusion flux component of m_k.

Hexahedral cells were generated by an automatic mesh generation tool, Pro-Modeler 2003 (CD-adapco Japan Co., LTD). The total number of cells used is 2 740 736. The maximum length of the cell is about 50 cm and the minimum length is 1 cm near the releasing source of SF_6.

The convergence criterion of the flow field calculation was set to be 0.1% for the summation of the residuals. The total number

TABLE I
AIR FLOW RESISTANCE PARAMETER OF POROUS CELLS

	α_1	β_1	α_2	β_2	α_3	β_3
Perforated floor	1000	1000	1000	1000	50	50
FFU filter	1000	1000	1000	1000	30	30
Return filter	300	300	50	50	300	300
Porous screen of the model process chamber	1000	1000	1000	1000	42.92	9.7

of iterations to reach the flow field convergence is about 3000. For the transient calculation of the SF_6 concentration field, the time step is decided by the Courant number, C, which is calculated as

$$C = \frac{|\vec{V}|\Delta t}{l} \tag{6}$$

where $|\vec{V}|$ and l are the characteristic velocity and dimension, respectively. In this study, the time step was set to be 0.1 s.

Flow velocity on the walls of the cleanroom was set to be zero at the boundaries. The uniform velocity boundaries at the inlets and outlets were assumed to be the average values of the velocities measured at the door openings. At the inlet boundaries, k and ε were given as $k = 1.5 \times (UI)^2$ and $\varepsilon = C_\mu^{0.75} \times k^{1.5}/\ell$, where U is the inlet velocity (m/s), I is the turbulent intensity, and ℓ is the turbulence length scale (m). In this study, ℓ was set to be 0.1. The exhaust flow rates drawn from the machine tools were set to be 60% and 40% at the outlet boundaries of the fab and sub-fab, respectively, according to the flow rates measured at the general ventilation ducts connecting to the exhausts of the tools.

The FFU cells in the model were treated as momentum sources based on the measured velocity data at 65 different regions as mentioned previously. The properties of the porous cells at four positions of the cleanroom were used to model the airflow resistance. The first position is the perforated floor, the second is the filters of FFUs, the third is the return filters and the forth is the porous screen on the model process chamber. The airflow resistances ΔP in these units can be expressed as [12]:

$$\Delta P = \alpha_i u_n^2 + \beta_i u_n \tag{7}$$

where subscript $i = 1, 2, 3$ corresponds to x, y, z directions, respectively; α and β are parameters related to inertia and viscosity, respectively; u_n is the superficial velocity normal to the surface of porous media. α and β can be calculated based on (7) from the pressure drop versus flow velocity data measured in this study or provided by the manufacturer and the values are shown in Table I.

IV. RESULTS

Experimental data of the gas concentration at the same locations were repeated and compared for precision. The comparison shows that the difference of the maximum peak concentration is less than 1.4% and the correlation coefficient of two repeated gas concentration distributions is higher than 0.91. It means that the present experiment has good precision. The simulated vertical velocities at 0.3 m below the FFUs are in good agreement with the measured data in 65 regions the FFUs. The maximum difference between the measured and simulated velocities is only 3.74%. In this clean room, air velocity averages about 0.27 m/s in the working zones and 0.55 m/s in the maintenance zones.

Fig. 6 shows the comparison of the experimental SF_6 concentrations with the simulated results at six different measurement points for the scenario A. Good agreement is seen with a maximum difference in the peak concentration of $< 36\%$. The comparison at other locations is similar except at point 2, which is very close to the SF_6 release location (the distance is only 3.7 m). SF_6 was released from a model chamber for 10 min to simulate the PM process which caused the concentration to increase in the clean room. The maximum SF_6 concentration appears at about 1000 s (or 16.6 min) which is several minutes after SF_6 release stops and then SF_6 continues to persist in the clean room for nearly another 40 min until its concentration drops to the background value.

Fig. 7 shows SF_6 dispersion patterns in the etching/thin-film area at 1 m above the perforated floor for scenario A. The concentration distribution is very nonuniform and it increases with SF_6 releasing time. The highest SF_6 concentration appears near the releasing model chamber at all times and it peaks at the 15th minute. The second highest SF_6 concentration region appears in the return duct with a maximum concentration of 158 ppb at the 15th minute. Fig. 8 further shows the side views of the SF_6 dispersion patterns in the maintenance area between D and E working zones (cross section $A - A'$ of Fig. 3). These figures indicate that SF_6 is drifted downward quickly by the flow of the FFUs. After passing through the perforated floor, SF_6 is flowing rapidly near the top regions of the sub-fab to the recirculation duct and accumulates in the supply air plenum. The pollutant is then dispersed in the clean room quickly. Since the clean room air flow must go through the recirculation duct, which results in high pollutant concentration to exist in the duct, the recirculation duct appears to be a good location to set up the gas sensors to detect the pollutant as quickly as possible.

V. DISCUSSION

A. Dilution Factor of the Cleanroom Air

Based on this study, the characteristic of the pollutant dispersion at various locations of the clean room is discussed in light of the maximum attainable concentration and dispersion time. A summary of the experimental data at different measurement points in the cleanroom is listed in Table II during the 10-min SF_6 release at the rate of 492 g/h. In the table, $C_{\max}$ is the maximum SF_6 concentration, $t_{\max}$ is the time for $C_{\max}$ to appear, and $t_{10\%}$ is the time required for SF_6 concentration to drop from its maximum value to 10% of the maximum value. The dilution factor is defined as the ratio of the released SF_6 concentration, or 100%, to $C_{\max}$. As shown in the table, the maximum value of the $C_{\max}$ appears at point 2, 4939 ppb, since it is closest to the release point. The corresponding dilution factor is 2.0×10^5, while the minimum value of $C_{\max}$ appears at point 20 is 50 ppb, and the corresponding dilution factor is 2.0×10^7. The dilution factor of the cleanroom air varies from 2.0×10^5 to 2.0×10^7 with the average value of 8.8×10^6. If point 2 is excluded, which is close to the releasing point, the range of the dilution factor is 1.0×10^6–2.0×10^7 with the average of 9.2×10^6. This value is close to 5.0×10^6, which is calculated based on the maximum

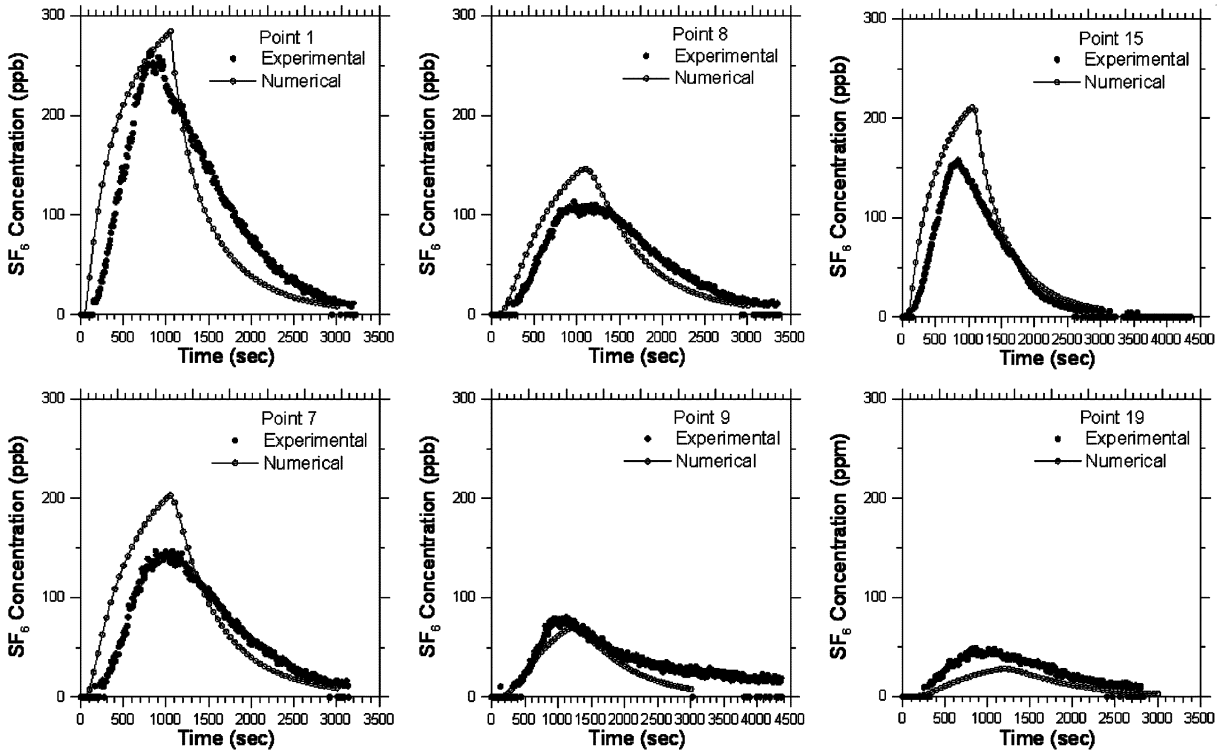

Fig. 6. Comparison of experimental SF_6 concentrations with simulated results at different locations, scenario A.

concentration predicted by the well-mixed model, 199.5 ppb, as will be shown in Section V-B. That is, when a gaseous pollutant is emitted to the cleanroom, the concentration of the pollution will be diluted to a large extent, which is about 10^5–10^7 if the emission time is 10-min and the emission rate is 492 g/hr.

Because of high dilution capacity of the cleanroom air, the toxic gas sensors in the clean room may not be able to set off the alarm for the concentration to exceed the permissible exposure limit (PEL). For example as shown in Table III, when SiH_4 of 1000 ppm leaks from a pipe at 492 g/h for 10 min, the maximum SiH_4 concentration detected will be 1 ppb, which is much less than its PEL of 5 ppm. As many of the alarm limits are set at the PELs, most toxic gas sensors will never be activated unless the leak is much serious or very close to the gas sensors, or the PELs are low (e.g., Cl_2 and ClF_3)

Therefore, a gas monitor with low detection limit is needed to protect the workers from injury. Similar or even lower detection limit of the gas monitors is needed to ensure a good product yield. These commercially available monitors include ion mobility spectroscopy (IMS), total molecular base real time monitor (TMB-RTM), and some nonselective AMC monitors [14]. However, these monitors are expensive and cannot monitor multipoints at the same time, a better monitoring strategy seems to be more desirable. One good monitoring strategy of AMCs is to monitor the recirculation air continuously as this study shows. The gas leak detection system (GLDS) composing of open-path FTIRs installed at the make-up air and recirculation air units was demonstrated to be a great tool for locating the leaking spot from thousands of pipelines [1]. With the GLDs system, the fab engineers could efficiently reduce contamination emissions and avoid their adverse effects on wafer defects, facilities, products, and personnel.

Table II furthers shows that after the maximum SF_6 concentration is detected, it takes an average of 24.6 min ($T_{10\%}$ range: 10–30.5 min) for the concentration to drop to 10% of its maximum value. This result is useful for the emergency response center (ERC) to formulate an evacuation procedure in the interest of time.

It is to be noted that the above discussion is based on the dilution factor calculated using the present experimental condition. The dilution factor is subjected to change when the emission rate and the emission time of the pollutant are different, as will be discussed further in Section V-B.

B. Nonuniformity of Gas Pollutant Distribution

The indoor air model was used to further characterize the dispersed pollutant concentration. Based on the mass conservation principle, the species concentration can be calculated as

$$V\frac{dC_i}{dt} = kq_0C_o\left(1-F_0\right) + kq_1C_i\left(1-F_1\right) + kq_2C_o - k\left(q_0+q_1\right)C_i + S \qquad (8)$$

where C is the concentration indoor (C_i) and outdoor (C_o); t is time; q is the volumetric flow rate for make-up air (q_0) and recirculation air (q_1), respectively; F is the filtration efficiency for make-up air (F_0) and recirculation air (F_1), respectively; V is the room volume; S is the indoor source emission rate; k is the factor characterizing the mixing condition ($k = 1$ for well-mixed condition). Based on (8) and assuming well-mixed condition, the maximum concentration was calculated to be 199.5 ppb. This well-mixed value was used to calculate the nonuniformity factor, which is defined as the ratio of the measured maximum concentration to 199.5 ppb. The calculated nonuniformity factor in Table IV shows that the factor

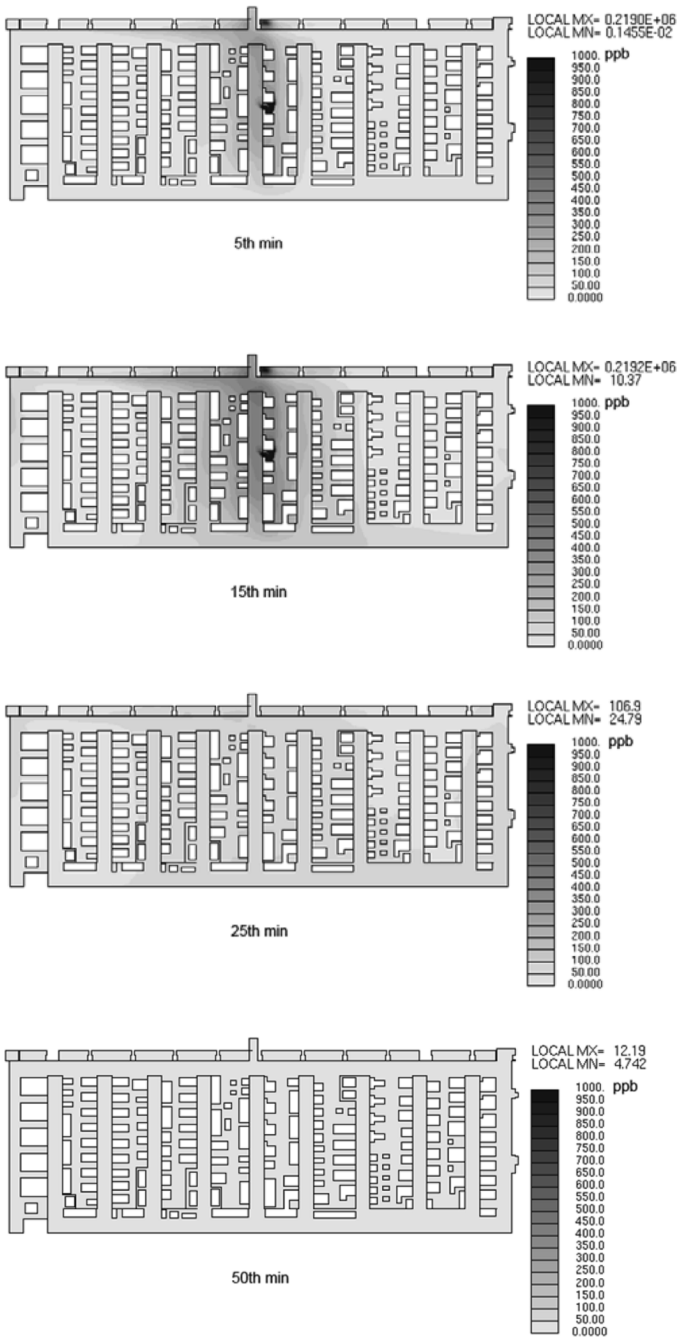

Fig. 7. SF_6 dispersion patterns in the etching/thin-film area of the fab layer, scenario A.

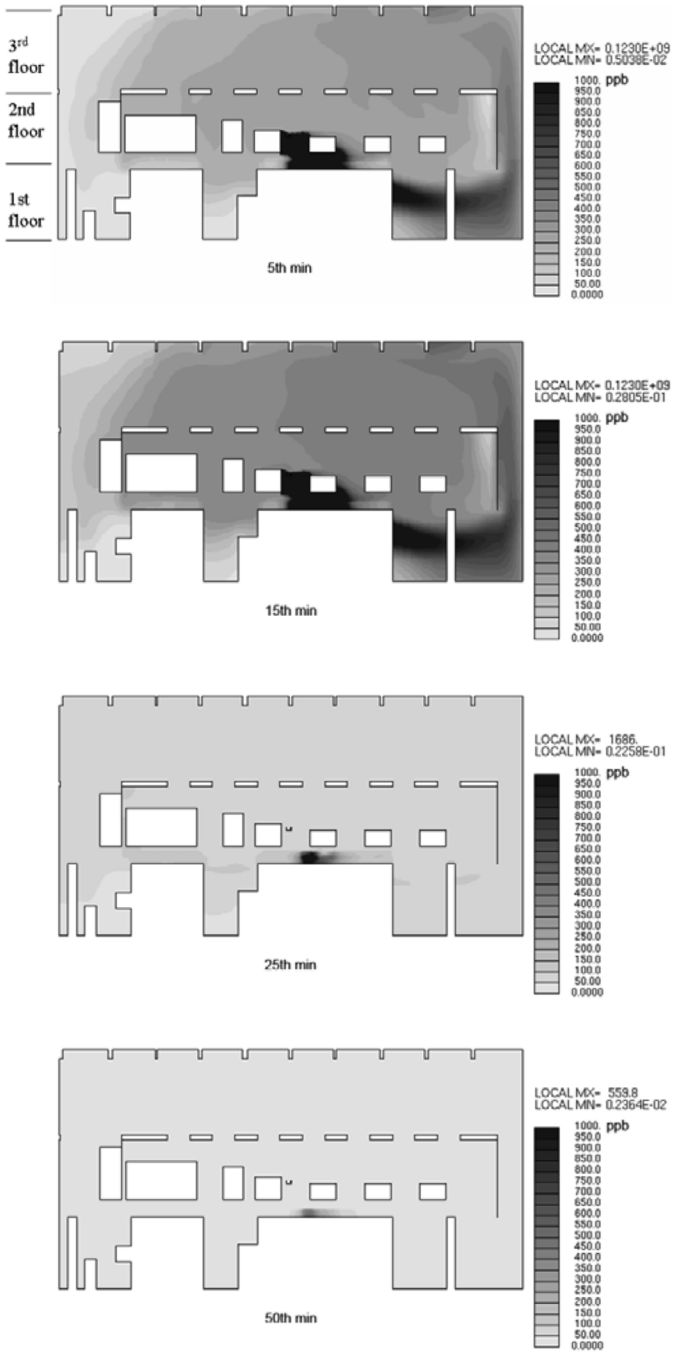

Fig. 8. SF_6 dispersion patterns in the cross section $A-A'$ of Fig. 3, scenario A.

decreases with an increasing distance from the sampling point to the SF_6 releasing source, and it ranges from 0.34 to 1.33 except point 2, which is very close to the releasing source. That is, the well-mixed model is useful for estimating an attainable maximum concentration value once a pollutant leaks in the cleanroom.

Fig. 9 shows the SF_6 concentration calculated by the well-mixed model and the simulated value at point 1 at different air exchange rates. It is seen that the well-mixed model predicts the maximum SF_6 concentration within a reasonable range. The predicted peak concentrations of 199.5 and 160.2 ppb are similar to the simulated values of 284.4 and 170.3 ppb for the air exchange rate of 4.7 and 7.8 times/hr, respectively. However, the time to reach the maximum concentration is much shorter (or $t_{\max}$ is too short) and the drop from the peak concentration is too abrupt (or $t_{10\%}$ is too short) for both exchange rates. Increasing the air exchange rate from 4.7 to 7.8 times/h reduces the peak concentration by about 30%. That is, increasing the air exchange rate when a gas leak occurs is an effective way to remove the pollutant in the cleanroom once a gas leak occurs.

C. Cross Contamination in the Lithography Area

The additional open-path FTIR with a low detection limit of 0.4 ppb monitored the SF_6 concentration at 5-min interval for 80

TABLE II
CHARATERISTICS OF DISPERSED SF_6 CONCENTRATION
(EMISSION RATE: 492 g/h)

Scenario	No.	C_{max} (ppb)	Dilution Factor	T_{max} (min)	$T_{10\%}$ (min)	Location
A	1	264	3.8E+06	13.6	29.7	fab
	2	4939	2.0E+05	12.5	20.8	fab
	3	114	8.8E+06	16.6	31.8	fab
	4	238	4.2E+06	13.3	28.4	fab
	5	86	1.2E+07	16.1	23.9	fab
	6	231	4.3E+06	14.2	29.1	fab
	7	147	6.8E+06	14.6	33.5	fab
	8	113	8.8E+06	16.1	35.2	fab
	9	81	1.2E+07	18.6	NA[b]	fab
	10	104	9.6E+06	13	NA	fab
	11	82	1.2E+07	16.3	NA	fab
	12	86	1.2E+07	16.8	28.7	fab
	13	68	1.5E+07	27.7	NA	fab
	14	67	1.5E+07	27.7	NA	fab
	15	158	6.3E+06	14.1	24	sub-fab
	16	63	1.6E+07	32.7	NA	sub-fab
	17	86	1.2E+07	20.1	30.5	sub-fab
	18	654	1.5E+06	18.3	10.5	sub-fab
	10	50	2.0E+07	14.4	NA	sub-fab
	20	73	1.4E+07	18.6	NA	sub-fab
B	21	219	4.6E+06	11.5	15.9	Fab
	22	548	1.8E+06	11.3	10	Fab
	23	147	6.8E+06	10.8	16.3	Fab
	24	151	6.6E+06	13.6	25	sub-fab
	25	986	1.0E+06	8.6	NA	sub-fab
	26	72	1.4E+07	10.6	NA	sub-fab
	Ave.	378	8.8E+06[a]	16.2	24.6	

Note: a. average dilution factor is 9.2E+6 if point 2 is excluded.
b. NA: when the concentration is lower than the detection limit of 10 ppb and $T_{10\%}$ is not available.

TABLE III
GAS SENSORS AND DEFAULT ALARM SETPOINTS
(EMISSION RATE: 492 g/h)

Target gas	PEL (ppm)	alarm setpoint of the sensor (ppm)	Conc. of process gas (%)	Max. conc. with 10^6 dilution (ppm)	If the alarm activates when the gas leaks ?
AsH_3	0.05	0.05	1	0.01	No
BCl_3	5*	5	>99	0.99	No
BF_3	1*	3	>99	0.99	No
Cl_2	0.5	0.5	>99	0.99	Yes
ClF_3	0.1	0.3	>99	0.99	Yes
CO	35	25	>99	0.99	No
SiH_2Cl_2	5*	5	>99	0.99	No
F_2	1	1	1	0.01	No
HBr	3	3	>99	0.99	No
HCl	5	5	>99	0.99	No
HF	3	3	>99	0.99	No
CH_3OH	200	500	>99	0.99	No
NF3	10	10	>99	0.99	No
NH3	50	25	>99	0.99	No
PH_3	0.3	0.3	10	0.1	No
SiF_4	3*	3	>99	0.99	No
WF_6	3*	3	>99	0.99	No
SiH_4	5	5	>99	0.99	No
CH_4	15000	500	>99	0.99	No
H_2	12000	500	>99	0.99	No

*: ceiling limits

min at the recirculation duct of the lithography area for both scenarios A and B when SF_6 was released in the etching/thin-film area. Totally, 13 samples were taken. A typical SF_6 concentration variation with time in the duct is shown in Fig. 10 for the 10th sample. It is seen that the maximum concentration is 1.8 ppb and the effect of cross contamination lasts very long. It takes

TABLE IV
THE NONUNIFORMITY FACTOR IN THE ETCHING/THIN-FLIM AREA

Scenario	No.	C_{max} (ppb)	Nonuniformity Factor	Direct Distance from Source (m)
A	1	264	1.33	10.6
	2	4939	24.76	3.7
	3	114	0.57	10.9
	4	238	1.19	9.1
	5	86	0.43	6.7
	6	231	1.16	10.6
	7	147	0.74	8.9
	8	113	0.57	10.1
	9	81	0.4	15.2
	10	104	0.52	19.3
	11	82	0.41	29.3
	12	86	0.43	12.6
	13	68	0.34	23.7
	14	67	0.34	36.2

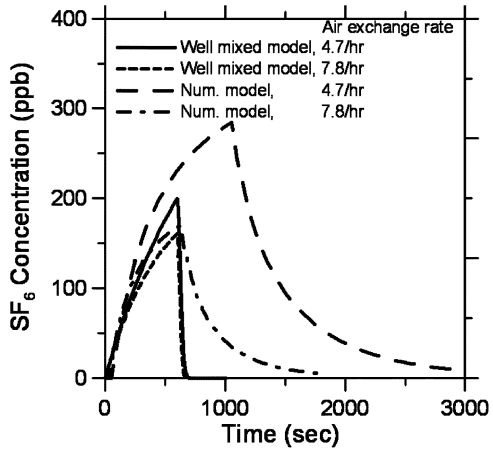

Fig. 9. Comparison of SF_6 concentration at different air exchange rates, point 1.

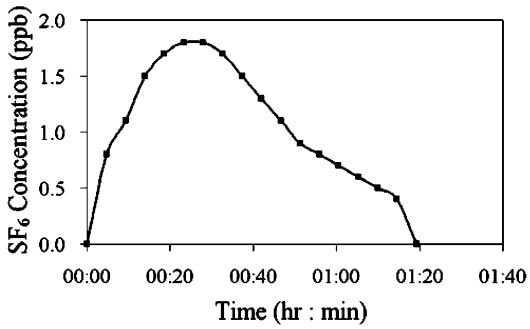

Fig. 10. A typical SF_6 concentration variatiocccn with time in the recirculation duct of the lithography area, 10th sample.

80 min from the time that SF_6 is detected until the concentration drops below the detection limit of 0.4 ppb.

The maximum 5-min average SF_6 concentration of all 13 samples are shown in Fig. 11, in which samples 1–11 were taken when the access door in the sub-fab layer between the lithography and thin film areas was normally closed, and samples 12–13 were taken when the door was always kept opened. Only samples 9–10 were taken for the scenario B while all the other samples were taken for the scenario A. Due to the process modifications in the lithography area, there was an unintended small slit (about 60 cm long by 1 cm wide) connecting the air plenum of the etching area to the fab level of the lithography area

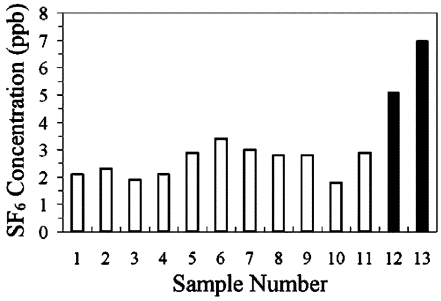

Fig. 11. The maximum 5-min average SF_6 concentration in the lithography area. Sample 1–11: door normally closed, 12–13: door normally open.

which allows air in the etching area to leak into the lithography fab area. But this small slit remained unnoticed by the lab personnel until the course of this experiment. This resulted in cross contamination even when the access door in the sub-fab was normally closed. For samples 1–11, the maximum SF_6 concentration measured in the recirculation duct ranges from 1.8 ppb to 3.4 ppb with an average of 2.6 ppb. When the access door in the sub-fab layer was always kept opened, SF_6 concentration was increased to more than two times, or 6.4 ppb, as shown in samples 12–13. Thus, door opening in the sub-fab layer can further enhance the cross contamination significantly in the lithography area from the pollutant in the etching/thin-film area.

In order to upgrade the process and increase the product yield, the modification of the process equipments and pipe lines is often necessary. Sometimes it will create an imperfectly isolated compartment such as the one found in this study. Without releasing the simulated pollutant and monitoring it continuously in the recirculation duct of the isolated lithography area, this unintended opening which leads to cross contamination problem will never be found. Besides process modifications, movement of operators, products and maintenance personnel across the access doors between different working areas will also lead to cross contamination and should be treated with great precaution.

REFERENCES

[1] S. N. Li, G. H. Leu, S. Y. Yen, S. F. Chiou, S. J. Yu, and C. F. Hsu, "Controlling contaminants with enhanced gas leak detection," *Solid State Technol.*, pp. 89–92, Jul. 2007.
[2] J. K. Higley and M. A. Joffe, "Airborne molecular contamination: cleanroom control strategies," *Solid State Technol.*, vol. 39, no. 7, pp. 211–212, Jul. 1996.
[3] D. Ruede, M. Ercken, and T. Borgers, "The impact of airborne molecular base on DUV photoresists," *Solid State Technol.*, vol. 44, no. 8, pp. 63–70, Aug. 2001.
[4] K. Kanzawa and J. Kitano, "A semiconductor device manufacturer's efforts controlling and evaluating atmospheric pollution," in *IEEE/SEMI Advanced Semiconductor Manufacturing Conf.*, 1995.
[5] S. N. Li, H. Y. Shih, Y. Y. Shaw, and J. Yang, "Case study of micro-contamination control," *Aerosol Air Qual. Res.*, vol. 7, no. 3, pp. 432–442, Sep. 2007.
[6] A. Shimazaki, H. Sakurai, K. Nishiki, and S. Nadahara, "Controlling Ru airborne contamination in cleanroom," in *2001 IEEE Int. Semiconductor Manufacturing Symp.*, Oct. 2001, vol. 8–10, pp. 333–336.
[7] S. N. Li, H. Y. Shih, K. S. Wang, K. Hsieh, Y. Y. Chen, Y. Y. Chen, and J. Chou, "Preventive maintenance measures for contamination control," *Solid-State Technol.*, vol. 48, no. 12, pp. 53–56, Dec. 2005.
[8] C. L. Chien, C. J. Tsai, K. W. Ku, and S. N. Li, "Ventilation control of air pollutant during preventive maintenance of a metal etcher in semiconductor industry," *Aerosol Air Qual. Res.*, vol. 7, no. 4, pp. 469–488, Dec. 2007.
[9] "Yield Enhancement," International Technology Roadmap for Semiconductors (ITRS) 2007.
[10] H. R. Shiu, H. Y. Huang, S. L. Chen, and M. T. Ke, "Numerical simulation for air flow in the mini-Environment and SMIF enclosure," *IEEE Trans. Semicond. Manuf.*, vol. 16, no. 1, pp. 60–67, Feb. 2003.
[11] S. C. Chen, C. J. Tsai, S. N. Li, and H. Y. Shih, "Dispersion of gas pollutant in a fan-filter-unit (FFU) cleanroom," *Buildg. Environ.*, vol. 42, no. 5, pp. 1902–1912, May 2007.
[12] *STAR-CD Version 3.24. Methodology*. London, U.K.: Computational Fluid Dynamics Software, Computation Dynamic Limited, 2004.
[13] S. V. Patankar, *Numerical Heat Transfer and Fluid Flow*. Bristol, PA: Hemisphere, 1980.
[14] R. Danfelt, *Real-Time Monitors: Review and Lithography Applications*, 27 ed. Belmont, CA: Semiconductor fabtech, pp. 100–106.

Hui-Ya Shih received her master degrees from the College of Engineering, National Chiao Tung University, Taiwan in 2007.

She is an associate researcher at the Energy and Environment Research Laboratories of the Industrial Technology Research Institute (ITRI), Taiwan.

Shih-Hsuan Huang received the master degrees from the Institute of Environmental Engineering, National Chiao Tung University, Taiwan, in 2005. He is a Ph.D. student in the Institute of Environmental Engineering, National Chiao Tung University, Taiwan, since 2005.

Shou-Nan Li received the Ph.D. degrees from the Department of Environmental Engineering Sciences, University of Florida, Gainesville, in 1999.

He is a senior researcher and department manager at the Energy and Environment Research Laboratories of the Industrial Technology Research Institute (ITRI), Taiwan. He leads a research team to develop the measurement and control technologies for the hazardous gases emitting from the hi-tech industries.

Sheng-Chieh Chen received the M.S. and Ph.D. degrees from the Institute of Environmental Engineering, National Chiao Tung University, Taiwan, in 2006.

He is a postdoc research fellow in the Institute of Environmental Engineering, National Chiao Tung University. His major research interest is flow modeling, particle control, and environmental nanoparticles.

Chuen-Jinn Tsai received the M.S. and Ph.D. degrees in the Particle Technology Laboratory (PTL), University of Minnesota, Minneapolis-St. Paul, in 1990.

He is a professor and chairman of the Institute of Environmental Engineering, National Chiao Tung University, where he has established the famous Nanoparticle and Air Quality Laboratory to conduct researches on aerosol sampling instruments, aerosol physics, aerosol control devices and air quality.